Journal of Hazardous Materials 182 (2010) 156–161

Contents lists available at ScienceDirect

Journal of Hazardous Materials

journal homepage: www.elsevier.com/locate/jhazmat

As(III) removal using an iron-impregnated chitosan sorbent

Daniel Dianchen Gang[a,*], Baolin Deng[b], LianShin Lin[c]

[a] Department of Civil Engineering, University of Louisiana at Lafayette, Lafayette, LA 70504, USA
[b] Department of Civil and Environmental Engineering, University of Missouri, Columbia, MO 65211, USA
[c] Department of Civil and Environmental Engineering, West Virginia University, Morgantown, WV 26506, USA

ARTICLE INFO

Article history:
Received 18 December 2009
Received in revised form 28 May 2010
Accepted 1 June 2010
Available online 9 June 2010

Keywords:
Trivalent arsenic
Iron-chitosan
Adsorption
As(III) adsorption kinetics
Adsorption isotherm

ABSTRACT

An iron-impregnated chitosan granular adsorbent was newly developed to evaluate its ability to remove arsenic from water. Since most existing arsenic removal technologies are effective in removing As(V) (arsenate), this study focused on As(III). The adsorption behavior of As(III) onto the iron-impregnated chitosan absorbent was examined by conducting batch and column studies. Maximum adsorption capacity reached 6.48 mg g^{-1} at pH = 8 with initial As(III) concentration of 1007 μg L^{-1}. The adsorption isotherm data fit well with the Freundlich model. Seven hundred and sixty eight (768) empty bed volumes (EBV) of 308 μg L^{-1} of As(III) solution were treated in column experiments. These are higher than the empty bed volumes (EBV) treated using iron-chitosan composites as reported by previous researchers. The investigation has indicated that the iron-impregnated chitosan is a very promising material for As(III) removal from water.

1. Introduction

Arsenic, resulting from industrial and mine waste discharges or from natural erosion of arsenic containing rocks, is found in many surface and ground waters [1]. Common chemical forms of arsenic in the environment include arsenate (As(V)), arsenite (As(III)), dimethylarsinic acid (DMA), and monomethylarsenic acid (MMA). Inorganic forms of arsenic (As(V) and As(III)) are more toxic than the organic forms [2]. Arsenite can be predominant in groundwater with low oxygen levels and is generally more difficult to be removed than arsenate [3]. Due to the negative impacts of arsenic on human health that range from acute lethality to chronic and carcinogenic effects, the U.S. Environmental Protection Agency revised the maximum contaminant level (MCL) of arsenic in drinking water from 50 to 10 μg L^{-1} [4]. This new regulation has posed a challenge for the research of new technologies capable of selectively removing low levels of arsenic.

Existing technologies that are being used for arsenic removal include precipitation [5], membrane separation, ion exchange, and adsorption [6–9]. While these approaches can remove arsenic to below 10 μg L^{-1} under optimal conditions, most of the systems are expensive, not suitable for small communities with limited resources. Of these methods, much work has been done on arsenic removal through adsorption because it is one of the most effective and inexpensive methods for arsenic treatment [7]. Therefore, development of highly effective adsorbents is a key for adsorption-based technologies.

Several iron(III) oxides, such as amorphous hydrous ferric oxide [5] and crystalline hydrous ferric oxide [10] are well known for their ability to remove both As(V) and As(III) from aqueous solutions. In general, arsenate is more readily removed by ferric (hydr)oxides than arsenite [11]. Reported mechanisms for arsenic removal include adsorption onto the hydroxide surfaces, entrapment of adsorbed arsenic in the flocculants, and formation of complexes and ferric arsenate ($FeAsO_4$) [12]. The presence of other anions such as sulfate, chloride, and in particular, silicates, phosphate, and natural organic matters, can significantly affect arsenic adsorption [13–15]. The use of iron (hydr)oxides in fine powdered or amorphous forms was found to be effective for arsenic removal, but the process requires follow-up solid/water separation. For packed-bed adsorption systems, high-efficient granular forms of adsorbent are essential.

Recently, several iron based granular materials and processes have been developed for arsenic removal. Dong et al. [16] developed iron coated pottery granules (ICPG) for both As(III) and As(V) removal from drinking water. The column tests showed that ICPG consistently removed total arsenic from test water to below 5 μg L^{-1} level. In another study, Gu et al. [17] used iron-containing granular activated carbon for arsenic adsorption. This iron-containing granular activated carbon was shown to remove arsenic most efficiently when the iron content was approximately 6%. Viraraghavan et al. [18] reported a green sand filtration process and found a strong correlation between influent Fe(II) concen-

* Corresponding author. Tel.: +1 337 4825184; fax: +1 337 4826688.
E-mail addresses: ddgang@louisiana.edu, digang@gmail.com, Gang@louisiana.edu (D.D. Gang).

0304-3894/$ – see front matter © 2010 Elsevier B.V. All rights reserved.
doi:10.1016/j.jhazmat.2010.06.008

tration and arsenic removal percentage. The removal percentage increased from 41% to above 80% as the ratio of Fe/As was increased from 0 to 20. Granular ferric hydroxide (GFH), another iron based granular material, showed a high treatment capacity for arsenic removal in a column setting before the breakthrough concentration reached 10 $\mu g\,L^{-1}$ [19]. It was found that complexes were formed upon the adsorption of arsenate on GFH [20]. Selvin et al. [21] conducted laboratory-scale tests over 50 different media for arsenic removal and found GFH with a particle size of 0.8–2.0 mm was the most effective one among the tested media. However, some disadvantages with GFH exist, including quick head loss buildup within 2 days because of the fine particle size, and significant reduction (50%) in adsorption capacity with larger sized media (1.0–2.0 mm).

Chitin and its deacetylated product, chitosan, are the world's second most abundant natural polymers after cellulose. These polymers contain primary amino groups, which are useful for chemical modifications and can be used as potential separators in water treatment and other industrial applications. Many researchers focused on chitosan as an adsorbent because of its non-toxicity, chelating ability with metals, and biodegradability [22]. Several studies have demonstrated that chitosan and its derivatives could be used to remove arsenic from aqueous solutions [23,24].

Based on the fact that both iron(III) oxides and chitosan exhibited high affinity for arsenic, this study focused on examining the effectiveness of an iron-impregnated chitosan granular adsorbent for arsenic removal. Most arsenic removal technologies are more effective for removing arsenate than for arsenite [12]. We found in this study that the iron-impregnated chitosan was effective for arsenite removal from experiments in both batch and column settings.

2. Experimental

2.1. Preparation of iron-chitosan beads

The experimental procedure for the preparation of iron-chitosan beads was described in detail by Vasireddy [25]. To summarize, approximately 10 g of medium molecular weight chitosan (Aldrich Chemical Corporation, Wisconsin, USA) was added to 0.5 L of 0.01 N $Fe(NO_3)_3{\cdot}9H_2O$ solution under continuous stirring at 60 °C for 2 h to form a viscous gel. The beads were formed by drop-wise addition of chitosan gel into a 0.5 M NaOH precipitation bath under room temperature. Maintaining this concentration of NaOH was critical for forming spherically shaped beads [25]. The beads were then separated from the 0.5 M NaOH solution and washed several times with deionized water to a neutral pH. The wet beads were then dried in an oven under vacuum and in air. The final iron content of the chitosan bead was about 8.4%.

2.2. Arsenic measurement

An atomic absorption spectrometer (AAS) (Thermo Electron Corporation) equipped with an arsenic hollow cathode lamp was employed to measure arsenic concentration. An automatic intermittent hydride generation device was used to convert arsenic in water samples to arsenic hydride. The hydrides were then purged continuously by argon gas into the atomizer of an atomic absorption spectrometer for concentration measurements.

As(III) stock solution (1000 $mg\,L^{-1}$) was prepared by dissolving 1.32 g of As_2O_3 (obtained from J.T. Baker) in distilled water containing 4 g NaOH, which was then neutralized to pH about 7 with 1% HCl and diluted to 1 L with distilled water. All the working solutions were prepared with standard stock solution. To 50 mL of each sample solution (i.e., reagent blank, standard solutions, and water samples), 5 mL 1% HCl and 5 mL of 100 $g\,L^{-1}$ NaI solution were used to convert arsenic in water samples to arsenic hydride.

2.3. Arsenic adsorption experiments

Each arsenic solution (100 mL) of desired concentration was mixed with the iron-chitosan beads in a 250 mL conical flask. The solution pH was adjusted with 0.1 M HCl or 0.1 M NaOH to obtain the desired pHs. A pH buffer was not used to avoid potential competition of buffer with As(III) sorption. One sample of the same concentration solution without adsorbent (blank), used to establish the initial concentration of the samples, was also treated under same conditions as the samples containing the adsorbent. The solutions were placed in a shaker for a fixed amount time, followed by filtration to remove the adsorbent. The filtrate was then analyzed for the final concentration of arsenic using the atomic absorption spectrometer. The solid phase concentration was calculated using the following formula:

$$q = \frac{(C_i - C_f)V}{M} \tag{1}$$

where, q ($\mu g\,g^{-1}$) is the solid phase concentration, C_i ($\mu g\,L^{-1}$) is the initial concentration of arsenic in solution, C_f ($\mu g\,L^{-1}$) is the final concentration of arsenic in treated solution; V (L) is the volume of the solution, and M (g) is the weight of the iron-chitosan adsorbent.

2.4. Kinetic experiments

Adsorption kinetics was examined with various initial concentrations at 25 °C. The pH of the solutions was chosen at 8.0 for optimal adsorption. The adsorbent loading for three different initial concentrations of 306, 584, and 994 $\mu g\,L^{-1}$ was all 0.2 $g\,L^{-1}$. A predetermined quantity of iron-chitosan adsorbent (20 mg) was placed in separate conical flasks with pH-adjusted As(III) solution. The conical flasks were covered with parafilm and placed in a shaker (150 rpm), and sub-samples of the solutions were then removed periodically and filtered prior to arsenic analysis.

To determine the reaction rate constants of arsenic adsorption onto iron-chitosan, both the pseudo-first-order and pseudo-second-order models were used. Kinetics of the pseudo-first-order model can be expressed as [26]:

$$\ln(q_e - q_t) = \ln\ q_e - k_1 t \tag{2}$$

where, k_1 (min^{-1}) is the rate constant of pseudo-first-order adsorption, q_t ($mg\,g^{-1}$) is the amount of As(III) adsorbed at time t (min), and q_e ($mg\,g^{-1}$) is the amount of adsorption at equilibrium. The model parameters k_1 and q_e can be estimated from the slope and intercept of the plot of $\ln(q_e - q_t)$ *vs* t. The pseudo-second-order model can be expressed as follow [27]:

$$\frac{t}{q_t} = \frac{t}{q_e} + \frac{1}{k_2 q_e^2} \tag{3}$$

where, k_2 ($g\,mg^{-1}\,min^{-1}$) is the pseudo-second-order reaction rate. Parameters k_2 and q_e can be estimated from the intercept and slope of the plot of (t/q_t) *vs* t.

2.5. Isotherm models

Adsorption isotherms such as the Freundlich or Langmuir models are commonly utilized to describe adsorption equilibrium. The Freundlich isotherm model is represented mathematically as:

$$q_e = k_f C_e^{1/n} \tag{4}$$

where, q_e ($mg\,g^{-1}$) is the amount of As(III) adsorbed, C_e ($\mu g\,L^{-1}$) is the concentration of arsenite in solution ($\mu g\,L^{-1}$), k_f and $1/n$

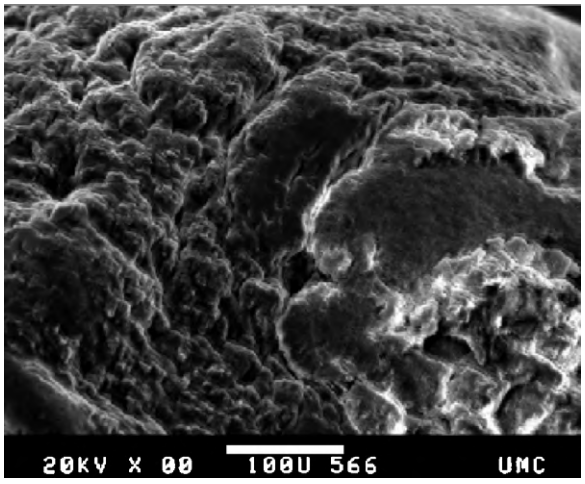

Fig. 1. Scanning electron micrograph (SEM) of iron-chitosan bead.

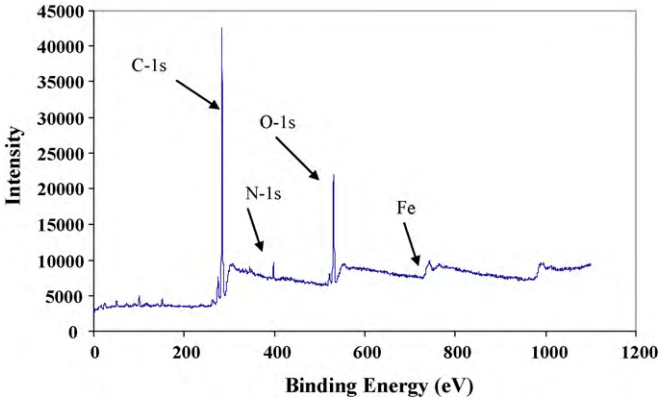

Fig. 2. XPS spectrum of iron-chitosan bead.

are parameters of the Freundlich isotherm, denoting a distribution coefficient ($L\,g^{-1}$) and intensity of adsorption, respectively. The Langmuir equation is another widely used equilibrium adsorption model. It has the advantage of providing a maximum adsorption capacity q_{max}($mg\,g^{-1}$) that can be correlated to adsorption properties. The Langmuir model can be represented as:

$$q_e = q_{max}\frac{K_L C_e}{1 + K_L C_e} \quad (5)$$

where, q_{max}($mg\,g^{-1}$) and K_L ($L\,mg^{-1}$) are Langmuir constants representing maximum adsorption capacity and binding energy, respectively.

2.6. Column study

Column study was conducted to investigate the use of iron-chitosan as a low-cost treatment technology for arsenite removal. Experiments were conducted with a 12-mm-ID glass column packed with 1.5 g iron-chitosan as a fixed bed. The influent solution had an inlet As(III) concentration of 308 $\mu g\,L^{-1}$ at pH 8, and was passed the column at a flow rate of 25 $mL\,h^{-1}$. Effluent solution samples were collected and analyzed for arsenic concentration during the column test.

3. Results and discussion

3.1. Structure characterization of iron-chitosan beads

The prepared iron-chitosan beads were examined by scanning electron microscope (SEM) (AMRAY 1600) for the surface morphology. A working distance of 5–10 mm, spot size of 2–3, secondary electron (SE) mode, and accelerating voltage of 20 keV were used to view the samples. It can be seen from Fig. 1 that the beads are porous in structure. X-ray Photoelectron Spectroscopy (XPS), a surface sensitive analytic tool to determine the surface composition and electronic state of a sample, was used in this study. In XPS analysis, a survey scan was used to determine the elements existing on the surface. The high resolution utility scans were then used to measure the atomic concentrations of Fe, C, N and O in the sample. Fig. 2 shows the peak positions of carbon, nitrogen, oxygen, and iron obtained by the XPS for iron-chitosan beads. In Fig. 2, the carbon 1s peak was observed at 283.0 eV with a FWHM (full width at maximum height) of 2.015. The Fe peak was observed at 730.0 eV. The N-1s peak for iron-chitosan bead was found at 398.0 eV (FWHM 2.00 eV), which can be attributed to the amino groups in chitosan.

3.2. Effect of pH

The effect of pH on arsenite removal with the iron-chitosan adsorbent was examined using100 mL As(III) solution with an initial concentration of 314 $\mu g\,L^{-1}$ and a solid loading rate of 0.15 $g\,L^{-1}$. The solution pH was adjusted with 0.1 M HCl or 0.1 M NaOH to obtain pHs ranging from 4 to 12. Lower pHs were avoided because the acid environments could lead to partial dissolution of the chitosan polymer and make the beads unstable [25,28]. The solutions were placed in a shaker (150 rpm) for 20 h at room temperature (25 °C), followed by filtration to remove the adsorbent. The amounts of As(III) adsorbed, calculated using Eq. (1), are present in Fig. 3. Under the experimental conditions, approximately 2.0 $mg\,g^{-1}$ of As(III) was adsorbed and that amount did not change significantly in the pH range 4–9. However, when pH was higher than 9.2, arsenite removal decreased dramatically with increasing pH.

The results can be explained using arsenic chemical speciation in different pH ranges [29]. Arsenite remains mostly as a neutral molecule for pH < 9.2, and negatively charged at pH > 9.2. So at pH > 9.2, arsenite sorption is less because of the unfavorable electrostatic interaction with negatively charged surfaces. This adsorptive behavior is common for arsenite with other adsorbents [17,30]. Gu et al. [17] reported that pH had no obvious effect on As(III) removal in the range of 4.4–9.0, with removal efficiency above 95%. Another study indicated that the uptake of As(III) by fresh and immobi-

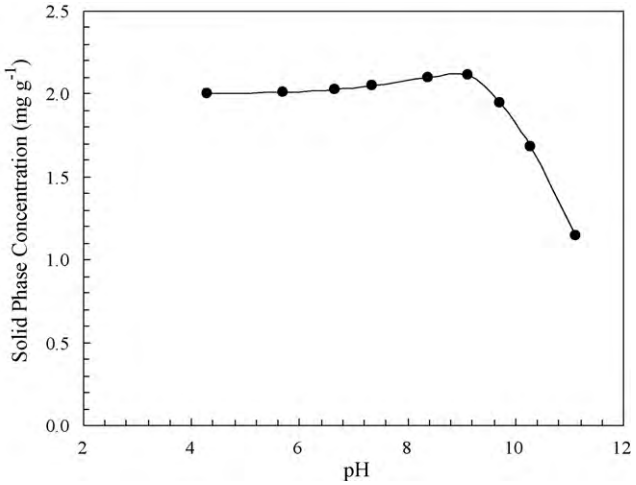

Fig. 3. Arsenite removal of the iron-chitosan adsorbent (0.15 $g\,L^{-1}$) as a function of pH for initial arsenite concentration of 314 $\mu g\,L^{-1}$ at T = 25 °C.

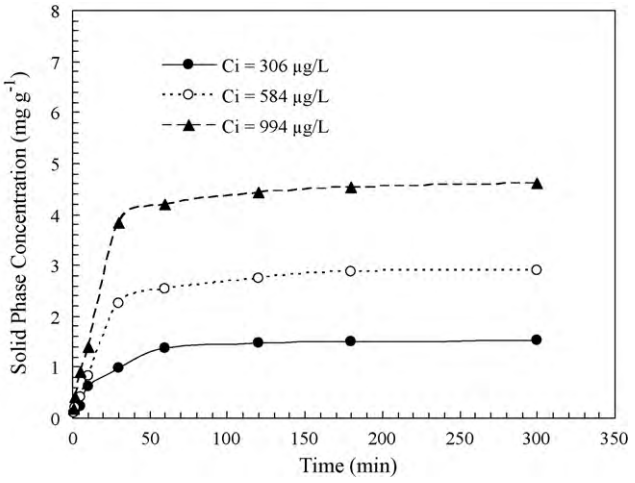

Fig. 4. Adsorption kinetics for different initial arsenite concentrations with iron-chitosan adsorbent loading of 0.2 g L^{-1} at pH = 8 and T = 25 °C.

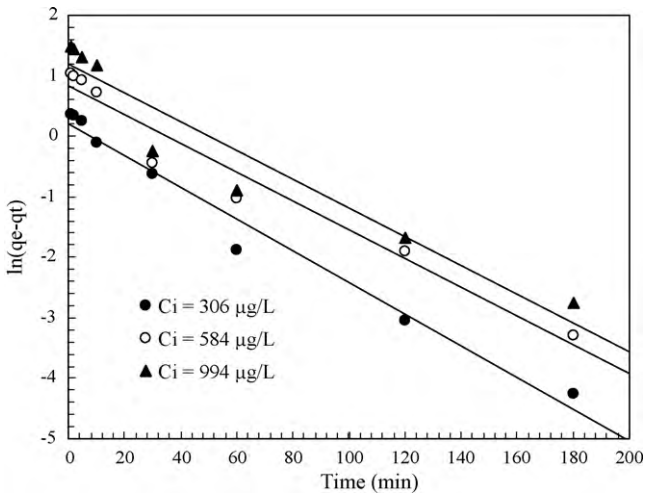

Fig. 5. Adsorption kinetics of the iron-chitosan adsorbent (0.2 g L^{-1}) for three initial arsenite concentrations at pH = 8 and T = 25 °C, and corresponding pseudo-first-order models.

lized biomass was not greatly affected by solution pH with optimal biosorption occurring at around pH 6–8 [30]. Raven et al. [11] reported that a maximum adsorption of arsenite on ferrihydrite was observed at approximately pH 9.

3.3. Kinetics of adsorption

Fig. 4 illustrates the adsorption kinetics for three different initial arsenite concentrations. More than 60% of the arsenite was adsorbed by iron-chitosan within the first 30 min, then adsorption leveled off after 2 h. Given the initial concentrations and adsorbent loading, equilibrium was reached after about 2 h. The adsorption capacity increased from 1.51 to 4.60 mg g^{-1} as the initial arsenite concentration was increased from 306 to 994 µg L^{-1}. The rapid adsorption in the beginning can be attributed to the greater concentration gradient and more available sites for adsorption. This is a common behavior with adsorption processes and has been reported in other studies [31]. The sorption rate of As(III) on naturally available red soil was initially rapid in the first 2 h and slowed down thereafter [32]. Elkhatib et al. [33] reported that the initial adsorption was rapid, with more than 50% of As(III) adsorbed during the first 0.5 h in an arsenite adsorption study. Fuller et al. [34] reported that As(V) adsorption onto synthesized ferrihydrite had a rapid initial phase (<5 min) and adsorption continued for 182 h. Raven et al. [11] studied the kinetics of As(V) and As(III) adsorption on ferrihydrite and found that most of the adsorption occurred within the first 2 h. It has been reported that arsenite forms both inner- and outer-sphere surface complexes on amorphous Fe oxide [35]. Another possible adsorption mechanism is hydrogen bond formation between As(III) and chitosan bead [24].

Figs. 5 and 6 illustrate model fits of the kinetic data for the pseudo-first-order and pseudo-second-order kinetic models. In general, the pseudo-second-order characterized the kinetic data better than the pseudo-first-order model. Table 1 summa-

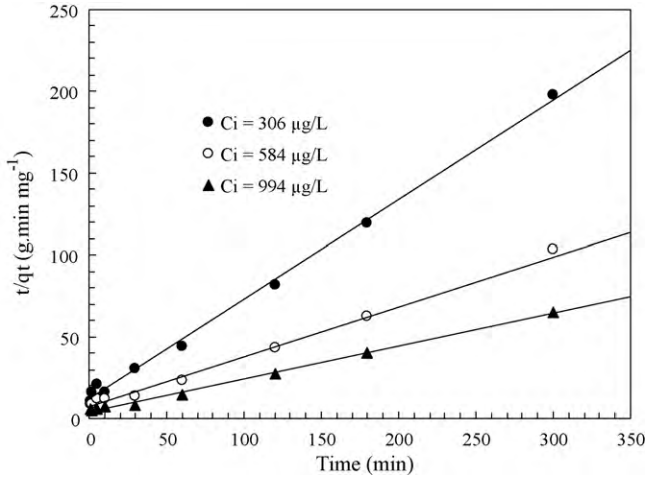

Fig. 6. Adsorption kinetics of the iron-chitosan adsorbent (0.2 g L^{-1}) for three initial arsenite concentrations at pH = 8 and T = 25 °C, and corresponding pseudo-second-order models.

rizes adsorption capacities determined from the model fits. It is noted that the second order rate constant (k_2) decreased from 3.19×10^{-2} to 1.15×10^{-2} g mg^{-1} min^{-1} as the initial concentration increased from 306 to 994 µg L^{-1}. The initial rate ($k_2 q_e^2$) increased from 8.48×10^{-2} to 27.97×10^{-2} with increasing initial As(III) concentration. Because as initial concentration increased, the concentration difference between the adsorbent surface and bulk solution increased.

Jimenez-Cedillo et al. [36] investigated arsenic adsorption kinetics on iron, manganese and iron-manganese-modified clinoptilolite-rich tuffs and concluded that the adsorption processes could be described by the pseudo-second-order model.

Table 1
Adsorption capacities and parameter values of kinetic models for three initial arsenite concentrations and iron-chitosan loading of 0.2 g L^{-1} at pH = 8.

Initial conc. (µg L^{-1})	Pseudo-first order				Pseudo-second order				
	$k_1 \times 10^2$ (min^{-1})	R^2	$q_{e,exp}$ (mg g^{-1})	$q_{e,col}$ (mg g^{-1})	$k_1 \times 10^2$ (g mg^{-1} min^{-1})	R^2	$q_{e,exp}$ (mg g^{-1})	$q_{e,col}$ (mg g^{-1})	$k_2 q_e^2 \times 10^2$
306	2.63	0.98	1.51	1.24	3.19	0.99	1.51	1.63	8.48
584	2.38	0.96	2.90	2.30	1.31	0.99	2.90	3.19	13.28
994	2.37	0.93	4.60	3.26	1.15	0.99	4.60	4.93	27.97

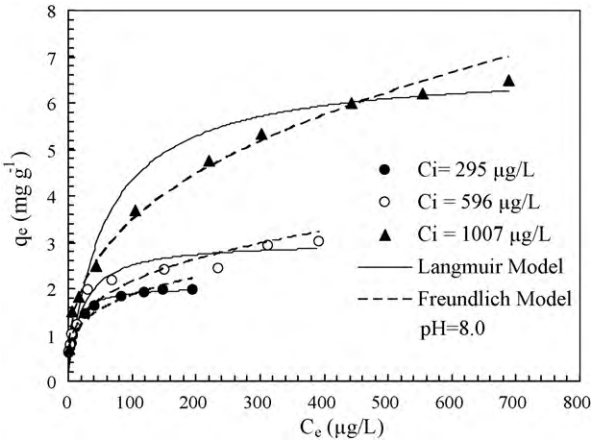

Fig. 7. Adsorption isotherms of the iron-chitosan adsorbent (0.2 g L^{-1}) for three initial arsenite concentrations at pH = 8, and corresponding isotherm models.

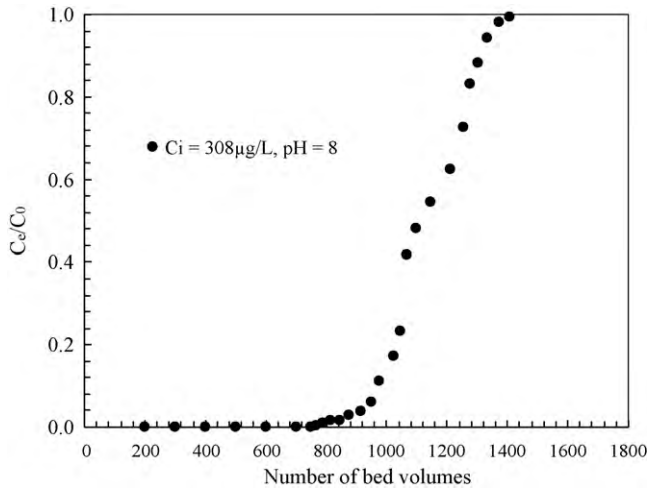

Fig. 8. Breakthrough curve for an inlet arsenite concentration of 308 μg L^{-1} at pH = 8 for a column reactor packed with the iron-chitosan adsorbent.

Thirunavukkarasu et al. [37] examined As(III) adsorption kinetics with granular ferric hydroxide (GFH) and found that most of As(III) adsorption onto GFH occurred at pH 7.6, with 68% of As(III) removed within 1 h and 97% removed at the equilibrium time of 6 h. Kinetic data fitted the pseudo-second-order kinetic model well with a kinetic rate constant of 0.003 g GFH h^{-1} μg^{-1} As, which is equivalent to 5.0×10^{-2} g mg^{-1} min^{-1} [37]. In our study, the kinetic rate constants were from 3.19×10^{-2} to 1.15×10^{-2} g mg^{-1} min^{-1}, which were smaller than using GFH. This could be attributed to the differences in adsorbent particle size and initial arsenic concentrations between these two studies.

3.4. Adsorption isotherms

Fig. 7 presents the adsorption isotherm data and two isotherm models at pH 8. The maximum adsorption capacity was found to increase from 1.97 to 6.48 mg g^{-1} as the initial concentration of As(III) increased from 295 to 1007 μg L^{-1}. Maximum adsorption capacity reached 6.48 mg g^{-1} with initial As(III) concentration of 1007 μg L^{-1}. Chen and Chung [24] reported that the adsorption capacity of As(III) was 1.83 mg As g^{-1} for pure chitosan bead. This study confirmed that impregnating iron into chitosan could significantly increase the As(III) adsorption capacity of the chitosan bead. In another study, Driehaus et al. [19] reported that the adsorption capacity could reach 8.5 mg As g^{-1} of granular ferric hydroxide (GFH). Model parameters and regression coefficients are listed in Table 2. The Freundlich model agreed better with the experimental data compared to the Langmuir model. The adsorption intensity ($1/n$) and the distribution coefficient (k_f) increased as the initial arsenite concentration increased. This indicated the dependence of adsorption on initial concentration. Low $1/n$ values (<1) of the Freundlich isotherm suggested that any large change in the equilibrium concentration of arsenic would not result in a significant change in the amount of arsenic adsorbed. Selim and Zhang [38] reported that adsorption isotherms of three different soils for As(V) were better fit to the Freundlich model and adsorption intensity values ranged from 0.270 to 0.340. Salim and Munekage [39] found that adsorptions of As(III) onto silica ceramic were well fit by the Freundlich isotherm. Similarly low $1/n$ values for As(V) adsorption have been reported by others [40].

3.5. Column study

Fig. 8 shows a breakthrough curve for an inlet arsenite concentration of 308 μg L^{-1} at pH 8. The break point was observed after 768 empty bed volumes (EBV) and adsorbent was exhausted at 1400 bed volumes. In comparison, Boddu et al. [23] reported that the break through point was about 40 and 120 EBV for As(III) and As(V), respectively using chitosan-coated biosorbent. Gupta et al. [41] conducted column tests using iron-chitosan composites for removal of As(III) and As(V) from arsenic contaminated real life groundwater. Their result showed that the iron-chitosan flakes (ICF) could treat 147 EBV of As(III) and 112 EBV of As(V) spiked groundwater with an As(III) or As(V) concentration of 0.5 mg L^{-1}. Given the difference of the initial concentrations between the two studies, the numbers of EBV were lower than what we found in this study. This can be partially attributed to the difference of the water constituents in the real grounder water used in the previous study [41].

Gu et al. [17] examined the arsenic breakthrough behaviors for an As-GAC sample prepared from Dacro 20 × 40 LI with an inlet concentration of 56.1 μg L^{-1} As(III). Their results demonstrated that the adsorbent could effectively remove arsenic from groundwater in a column setting. Dong et al. [16] also reported that average removal efficiencies for total arsenic, As(III), and As(V) for a 2-week test period were 98%, 97%, and 99%, respectively, at an average flow rate of 4.1 L h^{-1} and Empty Bed Contact Time (EBCT) >3 min.

Table 2
Values of the Freundlich and Langmuir isotherm model parameters for three arsenite concentrations with iron-chitosan loading of 0.2 g L^{-1} at pH 8.

Initial concentration (μg L^{-1})	Freundlich parameters			Longmuir constants		
	k_f (L g^{-1})	$1/n$	R^2	q_{max} (mg g^{-1})	K_L (L mg^{-1})	R^2
295	0.59	0.24	0.98	2.00	0.12	0.98
596	0.64	0.26	0.95	2.82	0.07	0.94
1007	0.74	0.33	0.99	6.82	0.01	0.95

4. Conclusions

Overall, the study has demonstrated that iron-impregnated chitosan can effectively remove As(III) from aqueous solutions under a wide range of experimental conditions and removal efficiency depends on various factors including pH, adsorption time, adsorbent loading, and initial concentration of As(III) in the solution. Results from the kinetic batch experiments indicated that more than 60% of the arsenic was adsorbed by the iron-chitosan within 30 min of adsorption. Kinetic results fit the pseudo-second-order model well. The second order reaction rate constants were found to decrease from 3.19×10^{-2} to 1.15×10^{-2} g mg^{-1} min^{-1} as the initial As(III) concentration increased from 306 to 994 μg L^{-1}. Adsorption isotherm results indicated that maximum adsorption capacity increased from 1.97 to 6.48 mg g^{-1} at pH = 8 as the initial concentration of As(III) increased from 0.3 to 1 mg L^{-1}. The adsorption isotherm data fit well to the Freundlich model. Column experiments of As(III) removal were conducted using 12-mm-ID column at a flow rate of 25 mL h^{-1} with an initial As(III) concentration of 308 μg L^{-1}.

This study corroborates that impregnating iron into chitosan can significantly increase As(III) adsorption capacity of the chitosan bead. Advantages of using the iron-impregnated chitosan include its high efficiency for As(III) treatment and low cost compared with the pure chitosan bead. We expect that the iron-impregnated chitosan is a useful adsorbent for As(III) and could be used both in conventional packed-bed filtration tower and Point of Use (POU) systems. The possible concerns include the physicochemical stability of the adsorbent because of the biodegradable nature of the chitosan material. Further research is underway to examine the adsorbent stability and whether the iron-impregnated chitosan can maintain its capability after several regeneration and reuse cycles. Competing adsorption of other ions will also be examined.

Acknowledgments

The authors would like to thank Mr. Ravi K. Kadari and Ms. Dhanarekha Vasireddy for conducting the laboratory experiments. The authors are grateful for financial support from the U.S. Department of Energy (Grant No.: DE-FC26-02NT41607).

References

[1] C.K. Jain, I. Ali, Arsenic: occurrence, toxicity and speciation, Water Res. 34 (2000) 4304–4312.
[2] W.R. Cullen, K.J. Reimer, Arsenic speciation in the environment, Chem. Rev. 89 (1989) 713–764.
[3] L. Dambies, Existing and prospective sorption technologies for the removal of arsenic in water, Sep. Sci. Technol. 39 (2004) 603–627.
[4] Fed. Regist. 67 (246) (2002) 78203–78209.
[5] M.B. Baskan, A. Pala, Determination of arsenic removal efficiency by ferric ions using response surface methodology, J. Hazard Mater. 166 (2009) 796–801.
[6] A.H. Malik, Z.M. Khan, Q. Mahmood, S. Nasreen, Z.A. Bhatti, Perspectives of low cost arsenic remediation of drinking water in Pakistan and other countries, J. Hazard Mater. 168 (2009) 1–12.
[7] D. Mohan, C.U. Pittman, Arsenic removal from water/wastewater using adsorbents—a critical review, J. Hazard Mater. 142 (2007) 1–53.
[8] V. Fierro, G. Muniz, G. Gonzalez-Sanchez, M.L. Ballinas, A. Celzard, Arsenic removal by iron-doped activated carbons prepared by ferric chloride forced hydrolysis, J. Hazard Mater. 168 (2009) 430–437.
[9] Y. Masue, R.H. Loeppert, T.A. Kramer, Arsenate and arsenite adsorption and desorption behavior on coprecipitated aluminum: iron hydroxides, Environ. Sci. Technol. 41 (2007) 837–842.
[10] X.Q. Chen, K.F. Lam, Q.J. Zhang, B.C. Pan, M. Arruebo, K.L. Yeung, Synthesis of highly selective magnetic mesoporous adsorbent, J. Phys. Chem. C 113 (2009) 9804–9813.
[11] K.P. Raven, A. Jain, H.L. Richard, Arsenite and arsenate adsorption on ferrihydrite: kinetics, equilibrium, and adsorption envelopes, Environ, Sci. Technol. 32 (1998) 344–349.
[12] J.G. Hering, M. Elimelech, Arsenic Removal by Enhanced Coagulation and Membrane Processes, AWWA Research Foundation, Denver, CO, 1996.
[13] D. Pokhrel, T. Viraraghavan, Arsenic removal from aqueous solution by iron oxide-coated biomass: common ion effects and thermodynamic analysis, Sep. Sci. Technol. 43 (2008) 3345–3562.
[14] B. Xie, M. Fan, K. Banerjee, J. van Leeuwen, Modeling of arsenic(V) adsorption onto granular ferric hydroxide, J. Am. Water Works Assoc. 99 (2007) 92–102.
[15] M. Jang, W.F. Chen, F.S. Cannon, Preloading hydrous ferric oxide into granular activated carbon for arsenic removal, Environ. Sci. Technol. 42 (2008) 3369–3374.
[16] L.J. Dong, P.V. Zinin, J.P. Cowen, L.C. Ming, Iron coated pottery granules for arsenic removal from drinking water, J. Hazard Mater. 168 (2009) 626–632.
[17] Z. Gu, F. Jun, B. Deng, Preparation and evaluation of GAC-based iron-containing adsorbents for arsenic removal, Environ. Sci. Technol. 39 (2005) 3833–3843.
[18] T. Viraraghavan, K.S. Subramanian, J.A. Arduldoss, Arsenic in drinking water-problems and solutions, Water Sci. Technol. 40 (1999) 69–76.
[19] W. Driehaus, M. Jekel, U. Hildevrand, Granular ferric hydroxide—a new adsorbent for the removal of arsenic from natural water, J. Water Serv. Res. Technol. 47 (1998) 30–35.
[20] X.H. Guan, J.M. Wang, C.C. Chusuei, Removal of arsenic from water using granular ferric hydroxide: macroscopic and microscopic studies, J. Hazard Mater. 156 (2008) 178–185.
[21] N. Selvin, G. Messham, J. Simms, I. Pearson, J. Hall, The development of granular ferric media—arsenic removal and additional uses in water treatment, in: Proceedings of Water Quality Technology Conference, Salt Lake City, UT, 2000, pp. 483–494.
[22] S. Hansan, A. Krishnaiah, T.K. Ghosh, Adsorption of chromium (VI) on chitosan-coated perlite, Sep. Sci. Technol. 38 (2003) 3775–3793.
[23] V.M. Boddu, K. Abburi, J.L. Talbott, E.D. Smith, R. Haasch, Removal of arsenic(III) and arsenic(V) from aqueous medium using chitosan-coated biosorbent, Water Res. 42 (2008) 633–642.
[24] C.C. Chen, Y.C. Chung, Arsenic removal using a biopolymer chitosan sorbent, J. Environ. Sci. Health A 41 (2006) 645–658.
[25] D. Vasireddy, Arsenic adsorption onto iron-chitosan composite from drinking water, M.S. Thesis, Department of Civil and Environmental Engineering, University of Missouri, Columbia, MO, 2005.
[26] D. Sarkar, D.K. Chattoraj, Activation parameters for kinetics of protein adsorption at silica-water interface, J. Colloid Interface Sci. 157 (1993) 219–226.
[27] Y.S. Ho, G. Mckay, Pseudo-second order model for sorption processes, Process Biochem. 34 (1999) 451–465.
[28] E. Guibal, C. Milot, J.M. Tobin, Metal-anion sorption by chitosan beads: equilibrium and kinetic studies, Ind. Eng. Chem. Res. 37 (1998) 1454–1463.
[29] S.K. Gupta, K.Y. Chen, Arsenic removal by adsorption, J. Water Pollut. Control Fed. 50 (1978) 493–506.
[30] C.T. Kamala, K.H. Chu, N.S. Chary, P.K. Pandey, S.L. Ramesh, A.R.K. Sastry, K.C. Sekhar, Removal of arsenic(III) from aqueous solutions using fresh and immobilized plant biomass, Water Res. 39 (2005) 2815–2826.
[31] H.D. Ozsoy, H. Kumbur, Adsorption of Cu(II) ions on cotton boll, J. Hazard Mater. 136 (2006) 911–916.
[32] P.D. Nemade, A.M. Kadam, H.S. Shankar, Adsorption of arsenic from aqueous solution on naturally available red soil, J. Environ. Biol. 30 (2009) 499–504.
[33] E.A. Elkhatib, O.L. Bennett, R.J. Wright, Kinetics of arsenite adsorption in soils, Soil Sci. Am. J. 48 (1984) 758–762.
[34] C.C. Fuller, J.A. Davis, G.A. Waychunas, Surface chemistry of ferrihydrite. Part 2. Kinetics of arsenate adsorption and coprecipitation, Geochim. Cosmochim. Ac. 32 (1993) 344–349.
[35] S. Goldberg, C.T. Johnston, Mechanisms of arsenic adsorption on amorphous oxides evaluated using macroscopic measurements, vibrational spectroscopy, and surface complexation modeling, J. Colloid Interface Sci. 234 (2001) 204–216.
[36] M.J. Jimenez-Cedillo, M.T. Olguin, C. Fall, Adsorption kinetic of arsenates as water pollutant on iron, manganese and iron-manganese-modified clinoptilolite-rich tuffs, J. Hazard Mater. 163 (2009) 939–945.
[37] O.S. Thirunavukkarasu, T. Viraraghavan, K.S. Subramanian, Arsenic removal from drinking water using granular ferric hydroxide, Water SA 29 (2003) 161–170.
[38] H.M. Selim, H. Zhang, Kinetics of arsenate adsorption–desorption in soils, Environ. Sci. Technol. 39 (2005) 6101–6108.
[39] M. Salim, Y. Munekage, Removal of arsenic from aqueous solution using silica ceramic: adsorption kinetics and equilibrium studies, Int. J. Environ. Res. 3 (2009) 13–22.
[40] B.A. Manning, S. Goldberg, Arsenic(III) and arsenic(V) adsorption on three California soils, Soil Sci. 162 (1997) 886–895.
[41] A. Gupta, V.S. Chauhan, N. Sankararamakrishnan, Preparation and evaluation of iron-chitosan composites for removal of As(III) and As(V) from arsenic contaminated real life groundwater, Water Res. 43 (2009) 3862–3870.